Atmos. Chem. Phys., 11, 5685–5700, 2011
www.atmos-chem-phys.net/11/5685/2011/
doi:10.5194/acp-11-5685-2011

Atmospheric Chemistry and Physics

Better constraints on sources of carbonaceous aerosols using a combined ^{14}C – macro tracer analysis in a European rural background site

S. Gilardoni[1], E. Vignati[1], F. Cavalli[1], J. P. Putaud[1], B. R. Larsen[2], M. Karl[3], K. Stenström[4], J. Genberg[4], S. Henne[5], and F. Dentener[1]

[1]European Commission, Joint Research Center, Institute for Environment and Sustainability, Ispra, Italy
[2]European Commission, Joint Research Center, Institute for Health and Consumer Protection, Ispra, Italy
[3]NILU, Norwegian Institute for Air Research, Kjeller, Norway
[4]Lund University, Department of Physics, Division of Nuclear Physics, Lund, Sweden
[5]EMPA, Swiss Federal Laboratories for Materials Science and Technology, Dübendorf, Switzerland

Received: 30 November 2010 – Published in Atmos. Chem. Phys. Discuss.: 24 January 2011
Revised: 10 May 2011 – Accepted: 30 May 2011 – Published: 20 June 2011

Abstract. The source contributions to carbonaceous $PM_{2.5}$ aerosol were investigated at a European background site at the edge of the Po Valley, in Northern Italy, during the period January–December 2007. Carbonaceous aerosol was described as the sum of 8 source components: primary (1) and secondary (2) biomass burning organic carbon, biomass burning elemental carbon (3), primary (4) and secondary (5) fossil organic carbon, fossil fuel burning elemental carbon (6), primary (7) and secondary (8) biogenic organic carbon. The mass concentration of each component was quantified using a set of macro tracers (organic carbon OC, elemental carbon EC, and levoglucosan), micro tracers (arabitol and mannitol), and ^{14}C measurements. This was the first time that ^{14}C measurements covered a full annual cycle with daily resolution. This set of 6 tracers, together with assumed uncertainty ranges of the ratios of OC-to-EC, and the reference fraction of modern carbon in the 8 source categories, provides strong constraints to the source contributions to carbonaceous aerosol. The uncertainty of contributions was assessed with a Quasi-Monte Carlo (QMC) method accounting for the variability of OC and EC emission factors, the uncertainty of reference fractions of modern carbon, and the measurement uncertainty.

During winter, biomass burning composed 64 % (±15 %) of the total carbon (TC) concentration, while in summer secondary biogenic OC accounted for 50 % (±16 %) of TC. The contribution of primary biogenic aerosol particles was negligible during the entire year. Moreover, aerosol associated with fossil sources represented 27 % (±16 %) and 41 % (±26 %) of TC in winter and summer, respectively. The contribution of secondary organic aerosol (SOA) to the organic mass (OM) was significant during the entire year. SOA accounted for 30 % (±16 %) and 85 % (±12 %) of OM during winter and summer, respectively. While the summer SOA was dominated by biogenic sources, winter SOA was mainly due to biomass burning and fossil sources. This indicates that the oxidation of semi-volatile and intermediate volatility organic compounds co-emitted with primary organics is a significant source of SOA, as suggested by recent model results and Aerosol Mass Spectrometer measurements. Comparison with previous global model simulations, indicates a strong underestimate of wintertime primary aerosol emissions in this region. The comparison of source apportionment results in different urban and rural areas showed that the sampling site was mainly affected by local aerosol sources during winter and regional air masses from the nearby Po Valley in summer. This observation was further confirmed by back-trajectory analysis applying the Potential Source Contribution Function method to identify potential source regions.

Correspondence to: E. Vignati
(elisabetta.vignati@jrc.ec.europa.eu)

1 Introduction

During the last decade the impacts of atmospheric aerosol on climate and human health have led to more intensive efforts to characterize particulate matter (IPCC, 2007; Pope and Dockery, 2006; Nel, 2005). Long-term measurements have shown that in Ispra the European legislation has effectively

succeeded in reducing PM_{10} concentrations over the last decade (Gruening et al., 2009), while the relative contribution of carbonaceous aerosol to $PM_{2.5}$ increased (Yttri et al., 2009).

Carbonaceous aerosol is an ubiquitous and significant component of atmospheric aerosol; it accounts for 20 to 50 % of the $PM_{2.5}$ mass in urban and rural locations, and up to 70 % of the PM_1 mass (Zhang et al., 2007; Querol et al., 2009). In the following years strategies to mitigate carbonaceous aerosol emissions will be necessary to control and lower aerosol concentrations. To achieve this, a better knowledge of carbonaceous aerosol sources on a regional scale is mandatory.

Molecular and elemental tracers have been used to identify the contribution of one or several aerosol sources. However, tracer methods have not completely characterized organic aerosol and especially Secondary Organic Aerosol (SOA). Field measurements on global (Zhang et al., 2007) and European scale (Morgan et al., 2010; Lanz et al., 2010) have shown that oxygenated organic aerosol (OOA), of which a major fraction is SOA, composes on average 60 % of submicron organic mass in urban locations and 80 % downwind of urban areas.

Receptor models, like Chemical Mass Balance, apportion primary carbonaceous aerosol sources based on the knowledge of chemical profile of each single source and the unapportioned mass is then assigned to SOA (Stone et al., 2008; El Haddad et al., 2010). The uncertainty of this derived SOA concentration is therefore large because it is affected by the sum of each primary source uncertainties. Other authors use the elemental carbon (EC) to organic carbon (OC) ratio to account for SOA mass and then explain the remaining aerosol mass by tracer analysis (Docherty et al., 2008; Yu et al., 2009). This method assumes that OC is emitted only by combustion sources and that the OC to EC ratio of primary emissions is well-known (Yu et al., 2009). This last assumption is seldom justified, since literature OC to EC ratios range over one order of magnitude, and when the ratio is empirically measured, it might be affected by sampling artifacts, and might not represent the variety of carbon sources and meteorology (Lee et al., 2010).

Using a different approach, source apportionment studies have been integrated with ^{14}C measurements to distinguish fossil from non-fossil carbon (Currie, 1982; Szidata et al., 2004; Gelencser et al., 2007; Hodzic et al., 2010). Fossil carbon is produced by fossil material use like fossil fuel combustion and production, while non-fossil carbon refers to carbonaceous aerosol with contemporary origin, like biogenic aerosol or biofuel combustion aerosol.

The isotope ^{14}C is formed in the upper troposphere and layers above mainly following the absorption of cosmic ray-produced neutrons by nitrogen atoms (Lal and Peters, 1967). The ^{14}C produced is quickly oxidized to carbon dioxide which is taken up by plants through photosynthesis in the troposphere. Thus, ^{14}C is incorporated into all land-living organisms. When an organism dies, the exchange of carbon with the surrounding environments ends and the $^{14}C/^{12}C$ ratio starts decreasing following the slow radioactive decay (half-life of 5730 ± 40 years) of the ^{14}C isotope. This decay is slow compared to the life time of organisms, but it is fast compared to fossil material time scale. As a consequence, the $^{14}C/^{12}C$ ratio in fossil fuels is zero and the isotopic ratio of atmospheric aerosol depends on the relative contribution of fossil and non-fossil carbon and on the age of modern carbon sources.

When radiocarbon data are combined with tracer measurements, they can be used to discriminate anthropogenic from natural, and primary from secondary aerosols (Gelencser et al., 2007; Ding et al., 2008; Lee et al., 2010).

In this paper we present a source apportionment study, focused on carbonaceous aerosol, which combines macro-tracers (OC, EC, and levoglucosan), micro-tracers (arabitol and mannitol), and ^{14}C measurements to explain both primary and secondary components of atmospheric carbonaceous aerosol. Tracers were used to apportion primary carbon, while ^{14}C data allowed us to distinguish fossil from non-fossil carbon. Carbon associated with SOA was calculated by combination of primary/secondary and fossil/non-fossil data.

To solve the source apportionment problem using macro-tracers, micro-tracers, and carbon isotopic ratio we needed to know for each source the corresponding emission factors and the reference fraction of modern carbon corresponding to the non-fossil sources. Due to the large variability and uncertainty of these input parameters, we decided to use a statistical approach to determine the source composition that has the best agreement with the measurements. This study presents a similar approach to that suggested by Gelencser et al. (2007) and Szidat et al. (2009), who used Latin Hypercube Sampling to calculate a large number of combinations of the input variables. We implemented instead an algorithm based on Quasi-Monte Carlo simulations (Caflisch et al., 1998); this method does not require to define a-priori the number of combinations of input variables, but defines this number according to the convergence of the solutions. The algorithm gave us the option to define the probability distribution function of the input variables: for example, we used step functions to describe the variability of parameters and Gaussian functions to describe the variability of observations. Finally, the algorithm implemented in this work allowed us to vary the reference fraction of non-fossil carbon ($f_{M(nf)}$) depending on the value used for the reference fraction of biomass burning aerosol ($f_{M(bb)}$), which in turn depends on the age of the biomass burnt.

To the best of our knowledge, this was the first time that radiocarbon analysis and tracer measurements were applied to such a large dataset, covering a full seasonal cycle. This enhances the representativeness of results and the significance of seasonal differences. The QMC approach allowed the quantification of the carbonaceous aerosol sources, and

at the same time the effect of the input parameter variability on the uncertainty of the apportionment results.

2 Methods

2.1 Aerosol sampling

Aerosol sampling was performed at the Joint Research Centre station for atmospheric research in Ispra, at a background site located to the northwest edge of the Po Valley in northern Italy (45°48′52″ N, 8°38′410″ E, 209 m a.s.l.). The distance from major anthropogenic emission sources is larger than 10 km. The main urban areas around the site are Varese to the east (at 20 km), Novara to the south (at 40 km), and Milan to the south-east (at 60 km). The site was recently characterized and compared with other European rural and remote background sites, and it was categorized as a typical background site in an environment generally strongly affected by anthropogenic emissions (Henne et al., 2010).

The site has been running under the European Monitoring and Evaluation Program (EMEP) since 1985. Measurements include meteorological parameters, aerosol scattering and absorption, particle number size distribution, and gas-phase species concentration (O_3, SO_2, NO_x, and CO). Since 2000 aerosol mass, organic and elemental carbon, and major inorganic ions have been routinely measured in the aerosol phase. Results presented in this paper refer to carbonaceous aerosols collected during 2007; a subset of daily samples was used for further analysis of organic aerosol (see next section).

24-hour fine aerosol samples ($PM_{2.5}$) were collected daily from 08:00 a.m. at $1\,m^3\,h^{-1}$ on 47 mm quartz filters, and were stored at 4 °C until the analysis. Filters were not pre-heated prior to analysis. Filters were weighted before and after the exposure at 50 % and 20 % relative humidity in a controlled atmosphere glove box.

2.2 Carbonaceous aerosol measurements

One punch ($1\,cm^2$) of each quartz filter was analyzed to measure organic carbon (OC) and elemental carbon (EC) concentration. OC and EC were measured by thermal-optical analysis with a Sunset Laboratory dual optical carbonaceous analyzer (Birch and Cary, 1996); the thermal evolution protocol EUSAAR-1 was followed (Cavalli et al., 2010). Quality control was performed with routine measurements of samples prepared with standard sucrose solution and the instrument was periodically calibrated with CO_2.

A subset composed of 48 daily $PM_{2.5}$ aerosol samples was further analyzed to measure tracers of primary biomass burning (levoglucosan) and primary biogenic aerosol (arabitol and mannitol), and to measure ^{14}C content. The samples were chosen according to the following criteria: to represent both cold and warm season, to represent both week days and week–end days, and to have a total carbon (TC) loading large enough to perform tracer and ^{14}C analysis (larger than $3\,\mu g\,m^{-3}$).

Levoglucosan (1,6-anhydro-β,d-glucopyranose) has been measured in atmospheric aerosol where it has been identified as a prevalent organic compounds in smoke from biomass combustion (Fraser and Lakshmanan, 2000; Nolte et al., 2001; Zdráhal et al., 2002; Simoneit et al., 2004; Dixon and Baltzell, 2006). Although other sources have been discussed for atmospheric emissions of levoglucosan, such as combustion of lignites (Fabbri et al., 2009) and char/charcoal (Kuo et al., 2008), these are not relevant for the site of the present study. The correlation of levoglucosan with non-dust soluble potassium, an inorganic tracer of biomass burning ($r^2 = 0.73$), confirms that atmospheric degradation, if present, did not compromise the use of this marker as a specific tracer of biomass combustion.

Arabitol and mannitol have been proposed as tracers of fungal spore emissions, and thus of primary biological aerosol particles (PBAP), according to Bauer et al. (2008a). PBAP include viable organisms, dead cells and cell fragments, such as pollen, bacteria, spores, plant debris, and viruses. The size of biological particles ranges over three orders of magnitude. Pollen grains, fragments of plants and animals are typically larger than 10 µm and their contribution to fine aerosol is negligible; on the contrary, spores can be smaller than 10 µm, bacteria can be as small as 1 µm, and viruses range around 100 nm (Matthias-Maser and Jaenicke, 2000). The concentration of primary biogenic carbon has been quantified using cellulose as a tracer of vegetation debris (Sanchez-Ochoa et al., 2007) and saccharides as tracers of fungal spores (Bauer et al., 2008a,b; Jia et al., 2010). In the present study we quantified primary biogenic OC based on arabitol and mannitol concentration, assuming that fungal spores dominated PBAP. Nevertheless, it should be kept in mind that other PBAP could be present and this work calculated a lower estimate of primary biogenic OC.

It has been reported that saccharides (including arabitol) may be emitted during leaf burning, but not during wood burning (Schmidl et al., 2008b). In the area around Ispra, leaf burning could be associated to agricultural waste combustion, which would take place in fall. Since arabitol concentration peaked in March and April and was zero in fall, we excluded the influence of burning emissions on arabitol concentrations.

For the analysis of levoglucosan, arabitol, and mannitol a method was implemented, based upon positive electrospray ionization mass spectrometry (Wan and Yu, 2006). Punches of $2\,cm^2$ were extracted for 7 min by ultrasonic treatment in methanol. The solvent was evaporated to near dryness by a mild flow of N_2, and the residue was dissolved in 250 µl, water containing 18 % methanol and 2 mM aqueous ammonium acetate. Aliquots (50 µl) were analyzed by high performance liquid chromatography mass spectrometry (HPLC-MS) using a 25 cm × 4.6 mm Prevail Carbohydrate, 5 µm column and a Thermo Ion-trap atmospheric pressure LCQ mass spectrometer. The mobile phase was composed of 20 % 10 mM aqueous ammonium acetate, 8 % methanol, and 72 % water.

Arabitol, levoglucosan, and mannitol were analyzed as ammonium adducts $[M+NH_4]^+$ and quantified by comparison to external standards; signals used for their quantification were *m/z* 170, *m/z* 180, and *m/z* 200, respectively. The precision of the method was evaluated by multiple extractions and injections to be better than 10 %. There was no interference with other compounds with the exception of isomeric forms of levoglucosan, such as the monosaccharide anhydrides mannosan (1,6-anhydro-β,d-mannopyranose) and galactosan (1,6-anhydro-β,d-galactopyranose), whose contribution was proved to be lower than 10 % (Ma et al., 2010).

2.3 Radiocarbon measurements

The carbon isotopic ratio of the non-fossil carbon in atmospheric aerosol has been affected by the nuclear bombing tests that took place during the late 1950's and early 1960's. The ^{14}C level of atmospheric CO_2 almost doubled during the tests. Since the test ban in 1963, the atmospheric $^{14}C/^{12}C$ ratio has decreased due to the uptake of CO_2 in the oceans and the biosphere and due to fossil fuel ^{14}C-free CO_2 input. The bomb-pulse in atmosphere at clean-air sites at different latitudes has been extensively studied and monitored (Levin and Kromer, 2004; Levin et al., 2008). At present the atmospheric $^{14}CO_2$ is still elevated compared to the natural reference level; in 2006 the enrichment was about 5 % (Levin et al., 2008). Environmental ^{14}C measurements are often expressed as the ^{14}C activity of the sample related to that of the international standard for modern carbon (Currie et al., 1989). This ratio is called "fraction of modern carbon" and is denoted f_M. Since it refers to the period prior to the nuclear bombing test, its value can be larger than one. Instead, the term reference fraction of non-fossil carbon ($f_{M(nf)}$) indicates the factor needed to calculate the non fossil carbon concentration. $f_{M(nf)}$ corrects for the nuclear bomb enrichment and the different content of ^{14}C of biomass burning and biogenic aerosol: because of the older age of burnt wood, carbonaceous aerosol from biomass wood burning is more enriched in ^{14}C than biogenic aerosol associated with PBAP and biogenic SOA.

The same subset of 48 samples as used for the organic tracer measurements was analyzed for ^{14}C. Prior to the ^{14}C measurements, 50–150 µg of carbon were extracted from the part of the residual filter area according to the principles described by Genberg et al. (2010). The ^{14}C content was quantified using the Lund University single-stage accelerator mass spectrometer (SSAMS) facility (Skog, 2007; Skog et al., 2010). Results are expressed in units of fraction of modern carbon, f_M.

The concentration of non-fossil carbon was calculated as the fraction of modern carbon divided by the reference fraction of non fossil carbon ($f_{M(nf)}$), and multiplied by the concentration of carbon (TC).

2.4 Source apportionment problem

2.4.1 Sources of carbonaceous aerosols

Carbonaceous aerosol was described as composed of the following 8 categories: primary OC from biomass burning (POC_{bb}), EC from biomass burning (EC_{bb}), primary OC from fossil fuel burning (POC_{ff}), EC from fossil fuel burning (EC_{ff}), primary OC from biogenic sources (POC_{bio}), secondary OC from biomass burning (SOC_{bb}), secondary OC from fossil sources (SOC_{ff}), and secondary OC from biogenic sources (SOC_{bio}). We assumed that these categories include all major sources of carbonaceous aerosol at the study site.

POC_{bb} and EC_{bb} are emitted by combustion of biomass, that around Ispra includes wood burning for residential heating in winter and episodic agricultural waste burning at the beginning of fall. During incomplete combustion of biomaterial, such as wood for residential heating, pyrolytic processes may lead to the formation of a number of compounds deriving from cellulose such as levoglucosan. POC_{bb} was inferred from the concentration of levoglucosan and EC_{bb} was calculated assuming a constant EC to OC ratio for primary biomass burning emissions.

$$POC_{bb} = [\text{levoglucosan}] \cdot k_1 \quad (1)$$

$$EC_{bb} = \frac{POC_{bb}}{k_2} \quad (2)$$

where k_1 and k_2 are the OC to levoglucosan and OC to EC emission ratios of biomass combustion, respectively.

POC_{ff} and EC_{ff} are emitted directly from combustion of fossil fuel including residential heating in winter, traffic and industrial processes during the entire year. EC_{ff} was inferred from the total EC concentration after subtraction of EC_{bb}, while POC_{ff} was calculated from EC_{ff} using the expected OC to EC ratio for primary fossil fuel combustion emissions (k_3).

$$EC_{ff} = [EC] - EC_{bb} \quad (3)$$

$$POC_{ff} = EC_{ff} \cdot k_3 \quad (4)$$

POC_{bio} is the OC associated to fungal spores, whose concentration was quantified using arabitol and mannitol, saccharides composed respectively by 5 and 6 carbon atoms. The number of spores was calculated as the average number of spores derived from arabitol and mannitol concentrations, according to Bauer et al. (2008a). To calculate the concentration of POC_{bio} in fine particles ($PM_{2.5}$) the content of OC from a single spore was assumed constant and equal to 5.2 pg C spore^{-1} (k_4 in Eq. 5), corresponding to the lower bound reported for PM_{10} aerosol (Bauer et al., 2002).

The contribution of primary biogenic carbon was then calculated according to Eq. (5).

$$POC_{bio} = [\text{number of spores}] \cdot k_4 \quad (5)$$

SOC_{ff} and SOC_{bb} correspond to OC produced by the oxidation (e.g. through aging) of intermediate volatility (IVOC), semivolatile (SVOC), and volatile organic compounds (VOC) from anthropogenic activities (Robinson et al., 2007), while SOC_{bio} is produced by the oxidation of gas-phase biogenic precursors. SOC_{ff} was determined by subtraction of primary carbon associated with fossil sources (POC_{ff} and EC_{ff}) from the fossil carbon (FC).

$$SOC_{ff} = FC - POC_{ff} - EC_{ff} \quad (6)$$

with

$$FC = [TC] \cdot (1 - \frac{f_M}{f_{M(nf)}}) \quad (7)$$

where TC is total carbon and $f_{M(nf)}$ being the reference fraction of modern carbon in non-fossil aerosols.

Secondary organic carbon from modern sources (SOC_{bb} and SOC_{bio}) was calculated by the combination of the following two equations:

$$OC = POC_{ff} + POC_{bb} + POC_{bio} + SOC_{ff} + SOC_{bb} + SOC_{bio} \quad (8)$$

$$f_M \cdot [TC] = (POC_{bb} + SOC_{bb} + EC_{bb}) \cdot f_{M(bb)} + (POC_{bio} + SOC_{bio}) \cdot f_{M(bio)} \quad (9)$$

where $f_{M(bb)}$ and $f_{M(bio)}$ are the reference fraction of modern carbon in biomass burning aerosol and biogenic aerosol, respectively. $f_{M(bio)}$ is known from measurements of ^{14}C content in atmospheric CO_2 and it's equal to 1.05 (Levin et al., 2008) in 2006. The discrimination between SOC_{bio} and SOC_{bb} was based on the different reference fraction of biomass and biogenic carbon. Table 1 summarizes the list of acronyms introduced in this section and the corresponding meaning.

Table 1. List of acronyms used in the paper and the corresponding descriptions.

Acronym	Description
POC_{bb}	Biomass burning primary OC
SOC_{bb}	Biomass burning secondary OC
EC_{bb}	Biomass burning EC
POC_{bio}	Biogenic primary OC
SOC_{bio}	Biogenic secondary OC
POC_{ff}	Fossil primary OC
SOC_{ff}	Fossil secondary OC
EC_{ff}	Fossil fuel burning EC
$f_{M(nf)}$	Reference fraction of modern carbon of non-fossil aerosol
$f_{M(bb)}$	Reference fraction of modern carbon of biomass burning aerosol
$f_{M(bio)}$	Reference fraction of modern carbon of biogenic aerosol

Table 2. Variability ranges of the input parameters used in the Quasi Monte Carlo simulations.

Parameter	Lower bound	Upper bound
OC to levoglucosan ratio k_1	4	13
OC to EC ratio–bb k_2	1	20
OC to EC ratio–ff k_3	0.3	1.2
OC to spore number k_4	5.2*	5.2*
$f_{M(bb)}$	1.13	1.31
$f_{M(nf)}$	1.05	$f_{M(bb)}$

* unit is pg C spore^{-1}.

2.5 Solution of the linear equations

2.5.1 Quasi-Monte Carlo approach

To solve the system of linear equations reported in the previous paragraphs, the following input parameters are needed: OC to levoglucosan emission ratio of biomass burning (k_1), OC to EC emission ratio of biomass burning (k_2), OC to EC emission ratio of fossil fuel combustion (k_3), $f_{M(bb)}$, and $f_{M(nf)}$.

Due to their variability and uncertainty, it would not be defendable to use single values for these parmeters. Instead, we explored the parameter space using a Quasi-Monte Carlo (QMC) approach to solve the linear equations (Boyle and Tan, 1997), and the 5 input parameters were allowed to vary with a step function across the whole uncertainty range reported in Table 2. To take into account measurement uncertainty of EC, OC, f_M, levoglucosan, arabitol, and mannitol, Gaussian curves were used to simulate distributions of observations; mean and standard deviations of the Gaussian distributions were set equal to measured concentrations and uncertainties, respectively. The uncertainties of levoglucosan, arabitol, and mannitol were calculated with the error propagation formula and taking into account peak integration, calibration, dilution error, and method reproducibility. f_M uncertainty was quantified based on analytical uncertainty. The uncertainty of OC and EC was determined based on the method reproducibility (Birch and Cary, 1996), and averaged 7 % and 15 %, respectively. The EC uncertainty was equal to the highest estimate of the measurement artifact calculated for EUSAAR-1 protocol (Cavalli et al., 2010). Uncertainty associated to filter inhomogeneity was neglected. In fact, replicate TC measurements on 150 mm filters showed that the error associated to the filter homogeneity assumption was smaller than 4 %; for 47 mm filters (as the ones used in the present study), the uncertainty would be even smaller and thus negligible compared to measurement uncertainty.

In a classical Monte Carlo approach, a large number of combinations of the input parameters would be tested and their values would be chosen randomly across the whole variability range. Quasi-Monte Carlo methods reduce the number of combinations needed to represent the parameter space, thanks to the use of deterministic sequence of values uniformly, rather than randomly, dispersed throughout the parameter domain. In this study we used the Sobol algorithm (Sobol, 1967) to create a 10-dimension deterministic

sequence. Each point of the sequence, described by 10 coordinates, is a combination of 5 input parameters and 5 input observations that can be used to solve the system of linear equations.

The Sobol sequence is a low discrepancy series. This means that any additional point of the series keeps the distribution of sampling points uniform. Thus, we did not need to define a priori the number of sampling points, but we could optimize it to guarantee the solution convergence.

During each iteration of the set of equations a new combination of parameters was tested. The maximum number of iterations was set to 100 000 and the convergence was achieved when:

- the number of iterations was at least 10 000,
- the number of non-negative solutions was larger than 1000,
- and the solution estimate varied by less than 1 % during the last three iterations.

The QMC method allowed us to calculate for each source during a certain day more than 10 000 solutions, corresponding to more than 10 000 iterations. As an example, Fig. 1 shows the frequency distribution of QMC solutions corresponding to primary and secondary OC measured on 11 January 2007. For each daily sample and for each carbon source the probability distribution of the solutions was analyzed to record the 5th, 25th, 50th, 75th, and 95th percentile, as well as the arithmetic mean value.

Some combinations of parameters led to negative concentrations. Negative solutions were considered meaningful if they were within the blank noise level. To investigate the blank noise, we studied the distribution of QMC solutions for a model blank sample; the resulting solution frequency distributions were symmetrical around zero. For each carbon source, the minimum concentration with physical meaning was assumed equal to the 25th percentile of the blank solutions. Concentrations larger than the 25th percentile and smaller than the 75th percentile were considered equal to zero, while concentrations larger than the 75th percentile were considered real. Combinations of input parameters that led to solutions smaller than the 25th percentile were discarded.

2.5.2 Input parameter variability range

Literature data indicate that emission ratios depend on nature and properties of fuel and on combustion conditions (i.e. temperature, open burning, contained burning, technology for pollution abatement); in addition, the EC emission factors are further affected by the variability related to the specific measurement technique, which can differ widely (Hitzenberger et al., 2006). Since EC and OC used in this study were measured by thermal-optical technique, the emission ratios here considered include only literature studies

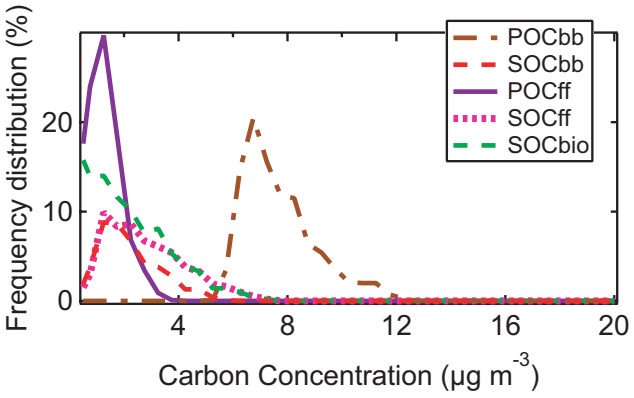

Fig. 1. Example of QMC solution frequency distributions corresponding to primary and secondary OC concentrations; EC frequency distributions are not reported for simplicity.

based on thermal-optical measurements, excluding absorption measurements, which would unrealistically widen the uncertainty.

The OC to EC ratios of fossil fuel burning strongly depends on the technology adopted for combustion and emission abatement. We consider here fossil fuel burning associated to transportation, residential heating, energy production, and industrial activities. Although the ratios reported in literature vary between 0.2 for boilers and heavy duty diesel vehicles and 6 for gas vehicles (Kupiainen and Klimont, 2004), values higher than 1.2 were measured only for vehicles used before 2000 (Watson and Chow, 2001; Kupiainen and Klimont, 2007). The variability range used in this study was 0.3–1.2; it comprises the ratio suggested for the overall fossil fuel consumption in western Europe (0.7) (Kupiainen and Klimont, 2007), as well as the emission ratio of vehicles in the Milan metropolitan area (60 km south of the sampling site) and measured from tunnel experiments (0.7) (Lonati et al., 2005).

OC and EC emission factors of biomass burning and fossil fuel combustion have been recently compiled in the IIASA interim report (Kupiainen and Klimont, 2004) and by the EPA SPECIATE4.1 program last updated in July 2008 (www.epa.gov/ttnchie1/emch/speciation). The compilation indicates that OC to EC ratios of biomass burning range between 0.5 and 69, depending on fuel type and burning conditions, with higher values for leaves and agricultural waste burning (Hays et al., 2002). The range used in the present study (1–20) corresponds to the range 5th–80th percentile of the literature ratios, and it is also in broad agreement with the range measured by Colombi et al. (2010) for wood and agricultural burning in northern Italy (1.7–20), which is likely representative for our measurement site.

The quantification of primary carbon in this study was based on emission factor ratios measured at relatively high dilution ratios compared to ambient conditions. For example,

the emission of carbonaceous aerosol from wood burning is usually determined at dilution ratios of 20 to 45 (Fine et al., 2001, 2002), while ambient conditions correspond to dilution of 1000–10 000. Robinson et al. (2007) showed that primary emissions evaporate significantly upon dilution and the gas-phase species formed by volatilization are then photo-oxidized to produce SOA. Since the majority of emission inventories available so far do not take into account the semivolatile character of primary emissions, the source apportionment results here presented might overestimate the effective primary pollution and underestimate by the same amount the corresponding secondary component.

The OC to levoglucosan emission ratios reported in literature range between 1.9 for fireplace combustion of eucalyptus logs (Schauer et al., 2001) and 28 for open burning of agricultural biomass (Hays et al., 2002). Most of the studies refer to wood species used for domestic heating in the United States (Fine et al., 2001, 2002, 2004) and only limited data exist for European emissions (Schmidl et al., 2008b,a). The emission ratios measured during burning of wood from central and southern Europe range between 3.7 and 12.7, while Puxbaum et al. (2007) recommend the interval 6–7 for contained combustion of European wood. In the present study the range 4–13 was employed.

$f_{M(nf)}$ could not be determined a priori since it depends on the relative contribution of modern carbon sources, e.g. biomass burning and biogenic aerosols, and their reference fractions of modern carbon $f_{M(bb)}$ and $f_{M(bio)}$. $f_{M(bio)}$ is 1.05, while $f_{M(bb)}$ depends on the age of the combusted material and the tree growth rate; literature studies (Lewis et al., 2004; Mohn et al., 2008) calculated that $f_{M(bb)}$ for wood harvested in 1999 and in 2005 are similar. Lewis et al. (2004) showed that, based on the model assumptions, $f_{M(bb)}$ can vary between 1.13 and 1.31. To account for this uncertainty range, $f_{M(bb)}$ and $f_{M(nf)}$ are used as input parameters in the QMC method: $f_{M(bb)}$ was let vary between 1.13 and 1.31, while $f_{M(nf)}$ was let to vary between 1.05 and the value assumed for $f_{M(bb)}$.

2.6 Atmospheric back-trajectories and PSCF analysis

To identify potential source regions for different aerosol fractions we combined the observations with atmospheric back-trajectory calculations. 5-day back-trajectories were calculated every 2 h for the sampling site using the trajectory model FLEXTRA (Stohl et al., 1995). The model was driven by 3-hourly European Center for Medium-range Weather Forecasts (ECMWF) analysis and forecast wind fields with $0.2° \times 0.2°$ horizontal resolution. Trajectories were initialized 50, 100, 200 and 500 m above model ground, to evaluate the uncertainty associated with vertical mixing at the measurement location. The atmospheric boundary layer height along the trajectory path was evaluated using the method described by Stohl et al. (2005). To account for additional vertical mixing in the Alpine terrain the envelope boundary layer height was used (Stohl et al., 2005).

The potential source contribution function (PSCF) (Zeng and Hopke, 1989) defines the probability for an aerosol source to be located in a certain geographical area described by a cell with coordinates (i, j). PSCF at (i, j) was calculated assuming that, if a back-trajectory passes through the atmospheric boundary layer of grid cell i, j, it picks up emissions from that area and transport them to the receptor site. To decide if a back-trajectory was within the atmospheric boundary at grid cell i, j the trajectory altitude was compared with the envelope boundary layer height and trajectory points outside the boundary layer were discarded. The function was defined by the ratio between the number of times that a back-trajectory associated with high concentrations passes through grid cell (i, j) $(m_{i,j})$ and the total number of times that back-trajectories pass through the grid cell (i, j) $(n_{i,j})$, according to the equation 10.

$$\mathrm{PSCF}_{i,j} = \frac{m_{i,j}}{n_{i,j}} \cdot w_{i,j} \tag{10}$$

The weight function $w_{i,j}$ was used to reduce the contribution from grid cells associated with low trajectory residence times (Pekney et al., 2004). The function $w_{i,j}$ was defined according to the following formula, where 40 was roughly equal to 3 times the standard deviation of $n_{i,j}$.

$$w_{i,j} = \begin{cases} 1 & \text{if } n_{i,j} \geq 40; \\ (\frac{n_{i,j}}{40})^3 & \text{if } n_{i,j} < 40; \end{cases}$$

Figure 2 shows for each $0.2° \times 0.2°$ grid cell the annual integrated number of back trajectory points within the boundary layer using 100 m as inizialitation altitude; regions affecting the sampling site include the Po Valley to the south – south east, the rural and marine area to the south, and Switzerland to the north, the latter corresponding to the Foehn conditions.

3 Results and discussion

3.1 Carbonaceous aerosol and tracers

Table 3 reports the average concentration and standard deviation of $PM_{2.5}$ mass, EC and OC corresponding to the daily aerosol samples collected from January till December 2007. The annual $PM_{2.5}$ average was higher than the target value of 25 $\mu g\,m^{-3}$ introduced by the European legislation in January 2010; the target value was exceeded 121 times during the year, indicating a strong influence of regional and local aerosol emission sources. The higher average values during winter (about three times higher than summer averages) were likely due to the contribution of residential heating and the lower mixing layer height that prevented pollutant dilution (Fig. 3a–b). Organic mass (OM) was calculated assuming an OM to OC ratio equal to 1.4; this value, which is close to the lower bound reported in literature (Turpin and Lim, 2001;

Table 3. Annual and seasonal average concentrations of $PM_{2.5}$, OC, EC, corresponding to the entire set of samples collected during 2007 (upper part) together with $PM_{2.5}$, OC, EC, levoglucosan, arabitol, and mannitol averages corresponding to the subset of 48 samples (lower part). Concentrations are in $\mu g\,m^{-3}$ and standard deviations are reported. Average values are calculated assigning one half of detection limit concentration to samples below detection limit (Antweiler and Taylor, 2008), and the number of samples with concentration above detection limit is reported between brackets.

Species	Entire year	Winter (Jan–Mar Oct–Dec)	Summer (Apr–Sep)
$PM_{2.5}$	25.7 ± 21.4 (322)	37.3 ± 23.6 (166)	13.5 ± 8.4 (156)
OC	9.2 ± 8.5 (334)	14.1 ± 9.2 (173)	4.0 ± 2.4 (161)
EC	2.3 ± 2.2 (334)	3.7 ± 2.3 (173)	0.9 ± 0.5 (161)
$PM_{2.5}$	35.9 ± 22.6 (49)	48.1 ± 27.3 (28)	19.6 ± 9.3 (21)
OC	13.8 ± 10.1 (49)	19.5 ± 10.2 (28)	6.3 ± 3.1 (21)
EC	3.5 ± 2.6 (49)	5.1 ± 13.0 (28)	1.4 ± 0.9 (21)
Levoglucosan	1.3 ± 1.8 (33)	2.1 ± 2.1 (28)	0.2 ± 0.2 (5)
Arabitol*	2.9 ± 6.0 (49)	4.4 ± 7.3 (12)	0.8 ± 2.3 (2)
Mannitol*	4.2 ± 9.8 (14)	6.3 ± 12.4 (12)	1.2 ± 1.8 (4)

* Arabitol and mannitol concentrations are in $ng\,m^{-3}$.

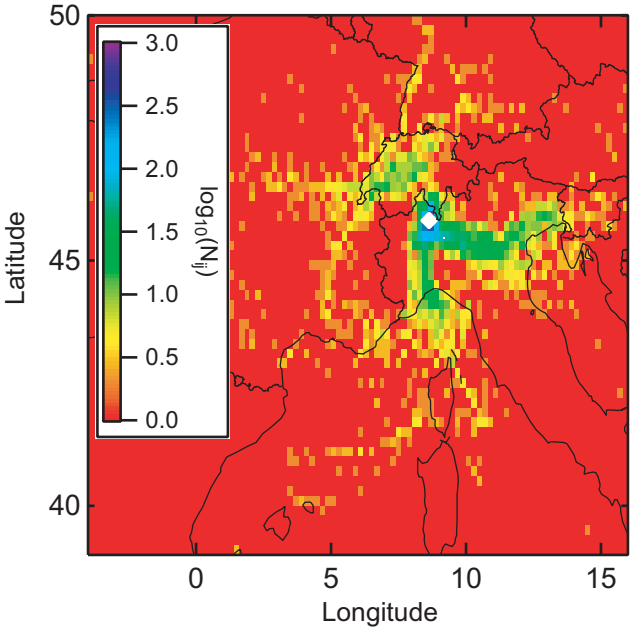

Fig. 2. Frequency distribution map (on a logarithmic scale) of back trajectory passes during aerosol collection periods.

Aiken et al., 2008), leads to a lower estimate of the OM contribution to fine aerosol mass. Nevertheless, OM represented 53 % and 41 % of fine mass during winter and summer, respectively, while the EC contribution was 10 % and 7 %.

The average $PM_{2.5}$ mass concentration, as well as the average EC and OC concentration for the subset of 48 samples

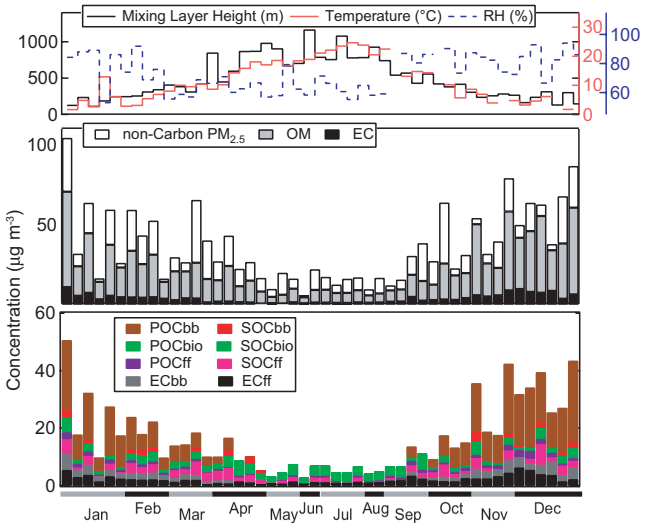

Fig. 3. Meteorological parameters **(a)**, contribution of OM and EC to $PM_{2.5}$ **(b)**, and best estimate results of source apportionment study **(c)** corresponding to the subset of daily aerosol samples here investigated.

(28 in winter and 20 in summer) selected for tracer and radiocarbon analysis were slightly larger than for the original data set. This was due to the selection criteria based on having enough carbonaceous aerosol to perform multiple tracer analysis and to overcome their detection limits. TC concentration of the subset of samples ranged from 3 to 53 $\mu g\,m^{-3}$, while the range corresponding to the entire dataset was 0.4–53 $\mu g\,m^{-3}$. The subset TC concentrations corresponded to the range 15th percentile–100th percentile, indicating that clean days were included in the source apportionment analysis, as well as polluted days. Student's t-test showed that the subset of samples was representative of the original data set with a 99 % significance level for $PM_{2.5}$ mass, OC, and EC.

$PM_{2.5}$ mass, OM, and EC daily concentrations of the subset of 48 samples are reported in Fig. 3b. The concentration of OM and EC averaged 19.4 $\mu g\,m^{-3}$ and 3.5 $\mu g\,m^{-3}$, respectively. The contribution of OM to $PM_{2.5}$ mass varied between 27 and 83 %, while EC fraction ranged between 3 and 22 %.

Levoglucosan (biofuel/waste burning tracer) was detected in all samples collected during the colder season, while during the warmer period only a small number of samples showed concentrations above detection limit, mainly collected at the beginning of spring and at the end of summer, when environmental conditions were dry enough to burn biomass waste. The average winter concentration in Ispra (2.1 $\mu g\,m^{-3}$) was higher than the values measured in continental and maritime background European sites (Puxbaum et al., 2007). However, it was comparable to the upper bound of the concentration range measured at European rural sites (i.e. K-puszta, Hungary, and Aveiro, Portugal) (Puxbaum et al., 2007). In relative terms, the

winter average contribution of levoglucosan to carbonaceous aerosol in K-puszta and Aveiro was 5 and 9 %, respectively (Gelencser et al., 2007), and it was 9 % in Ispra. The percentage contribution measured in the more urbanized Po Valley, at close distance (ca. 50 km) from the measurement site, in winter 2007 and 2009 was 5 % (B. R. Larsen, personal communication, 2010), indicating a larger use of wood for residential heating in rural region surrounding Ispra.

About one third of the samples was characterized by detectable amounts of saccharides (marker for PBAP), whose concentrations ranged between 2.6 and 31 ng m^{-3} for arabitol and from 2.3 to 52 ng m^{-3} for mannitol, with the highest values measured at the end of March. These concentrations were smaller than those reported by Bauer et al. (2008a) for an urban site in Vienna, Austria, for PM_{10} samples (arabitol: 7–63 ng m^{-3} and mannitol: 8.9–83 ng m^{-3}), consistently with a bimodal distribution of these species in fine and coarse particles (Kourtchev et al., 2009). The range of arabitol and mannitol concentrations measured in $PM_{2.5}$ aerosol at a rural site in Texas (Jia et al., 2010) were similar to those measured in Ispra.

3.2 Sources of carbonaceous aerosol

For each daily sample and for each carbon source the Quasi-Monte Carlo simulation calculated the frequency distribution of the solutions from all combinations of the input parameters. The 50th percentile of this distribution is here considered the best estimate of the carbon source strength. Figure 3c shows the best estimate results for the 8 carbon sources described in the experimental section. Note that the OC is not converted into organic mass so the plot does not account for the contribution of atoms other than carbon, which may add another 30–80 % to the carbon mass. Annual and seasonal average carbon concentrations are reported in Table 4.

The single most important carbonaceous aerosol source in Ispra was biomass burning. Although its presence was limited to the colder months, it represented 41 % of the total mass of carbon during the whole year. POC_{bb}, SOC_{bb}, and EC_{bb} accounted for 79 %, 6 %, and 15 % of the total biomass burning carbon, respectively. The highest concentrations were measured in January, November, and December, the coldest months of the year. In the study area the possible sources of biomass burning carbon are wildfires, agricultural waste burning, and wood burning for residential heating. The absence of this source during summer, when dryer weather conditions could facilitate wildfires in the surrounding regions, and the small concentrations during fall, when agricultural waste burning takes place, indicate that the main source of biomass burning carbon observed in Ispra was wood burning for residential heating. This conclusion was further supported by the observation that non-dust soluble potassium and levoglucosan concentrations correlated with a slope equal to 0.13, a value closer to fireplace and wood stove emission ratios rather than to open burning ratios (Puxbaum et al., 2007).

Table 4. Annual and seasonal average carbon concentrations (in μg m^{-3}) of the Quasi Monte Carlo best estimate results, and corresponding fraction of carbon mass between brackets.

Source	Entire year	Winter (Jan–Mar Oct–Dec)	Summer (Apr–Sep)
POC_{bb}	6.6 (31 ± 7 %)	11.9 (50 ± 10 %)	0.5 (5 ± 3 %)
SOC_{bb}	0.5 (3 ± 7 %)	0.8 (3 ± 8 %)	0.3 (3 ± 5 %)
EC_{bb}	1.3 (7 ± 5 %)	2.5 (11 ± 8 %)	0.2 (1 ± 2 %)
POC_{bio}	<0.1	<0.1	<0.1
SOC_{bio}	2.5 (26 ± 10 %)	2.0 (9 ± 12 %)	3.1 (50 ± 7 %)
POC_{ff}	0.9 (7 ± 6 %)	1.2 (5 ± 5 %)	0.6 (9 ± 7 %)
SOC_{ff}	1.6 (12 ± 13 %)	2.3 (10 ± 12 %)	1.3 (14 ± 15 %)
EC_{ff}	2.0 (15 ± 7 %)	2.6 (12 ± 8 %)	1.2 (18 ± 7 %)

Biogenic carbon was dominated by secondary sources. The contribution of POC_{bio} ranged between 5 and 110 ng m^{-3} and was negligible compared to SOC_{bio}, whose concentration ranged from values below 1 μg m^{-3} in winter up to 7.5 μg m^{-3} in spring. On average SOC_{bio} represented 9 % and 50 % of carbonaceous aerosol during winter and summer, respectively, while POC_{bio} contribution was less than 1 % in all samples.

Karl et al. (2009) used global chemistry transport model TM5 to evaluate the contribution of secondary biogenic aerosol at Ispra. We compared the result of this source apportionment study with the model output (Fig. 4). The SOC_{bio} in summer averaged 3.1 μg m^{-3}, corresponding to 5.6 μg m^{-3} of organic mass, calculated with the ratio OM to OC equal to 1.8 (Aiken et al., 2008); this concentration agrees well with the average secondary organic aerosol (SOA) concentration (5.4–5.8 μg m^{-3}) simulated by the TM5 during July 2002 in northern Italy (Karl et al., 2009). In addition to terpene oxidation, the model simulation includes the SOA derived from isoprene oxidation. SOA is described as an equilibrium partitioning of secondary biogenic species between gas and aerosol phase.

From May to August biogenic emissions of e.g. isoprene have been shown to peak at our measurement site (Duane et al., 2002). Daily samples collected during the same months showed that the mass fraction of biogenic secondary carbon (i.e. SOC_{bio} normalized to the fine aerosol mass) correlated very well with the mass fraction of primary carbon (i.e. the sum of primary OC and EC normalized to fine mass), that in summer is emitted almost exclusively by anthropogenic fossil sources. The normalization to fine mass is used to remove the effect of meteorology. SOC_{bio} has different sources (oxidation and aging of biogenic volatile precursors) compared to primary organic particles (combustion processes, transportation). PSCF (Sect. 3.6) indicates that the source region of the two carbon fractions are different:

primary fossil carbon is produced by local sources and emissions of urban and industrial areas in the nearby Po valley, while biogenic SOA is produced by oxidation of biogenic volatile compounds, likely originated in the rural area around the sampling site. In addition, the lack of correlation among other carbonaceous particle fractions indicates that residence time or similar history of carbonaceous particles is not enough to explain the relationship between biogenic secondary and primary OA. In conclusion, the good correlation between SOC_{bio} and primary carbon fractions ($r^2 = 0.79$) could be explained by the promotion of biogenic secondary aerosol formation by primary carbonaceous material. As suggested by Bowman and Melton (2004), a larger fractions of anthropogenic aerosol can offer a larger surface area with chemical affinity for condensation of biogenic gas phase precursors. A similar enhancement was predicted by CMAQ model in the eastern United States (Carlton et al., 2010).

Carbonaceous aerosol from fossil sources was observed both during winter and summer and composed on average 34 % of the total carbon mass. It partitioned into POC_{ff} (20 %), SOC_{ff} (36 %), and EC_{ff} (44 %). Differently from biomass burning, fossil fuel combustion produced a larger amount of elemental carbon relative to primary and secondary organic carbon. Although, the fraction of TC represented by fossil source aerosol was higher in summer than in winter, the average concentrations of POC_{ff}, SOC_{ff}, and EC_{ff} during winter were about twice the summer values.

3.3 Can source apportionment data explain model/observation disagreement?

The global chemistry transport model TM5 (Krol et al., 2005) was employed by Karl et al. (2009) to simulate OM concentration at Ispra during the EMEP intensive campaign from July 2002 to June 2003. Globally, a horizontal resolution of $6° \times 4°$ was used, with a two-way zooming algorithm resolving the European domain at a resolution of $1° \times 1°$. TM5 was coupled with the secondary organic aerosol module developed by Tsigaridis et al. (2006) and linked to the gas-phase chemistry module CMB-IV (Gery et al., 1989). The model underestimated the observation during most time of the year, with the exception of July - August period.

The average OC concentrations measured during the intensive campaign 2002/2003 (12.1 $\mu g\,m^{-3}$ in winter and 4.8 $\mu g\,m^{-3}$ in summer) were comparable to those measured during 2007 within the variability range. The similarity of carbonaceous aerosol concentrations observed during the two periods allowed the comparison of source apportionment results of 2007 with model simulation of 2002/2003.

The OM simulations were divided into POA and SOA contributions. For comparison purposes the measured POA and SOA were calculated according to the following equations:

$$POA = 1.4 \cdot POC_{bb} + 1.4 \cdot POC_{bio} + 1.4 \cdot POC_{ff} \quad (11)$$

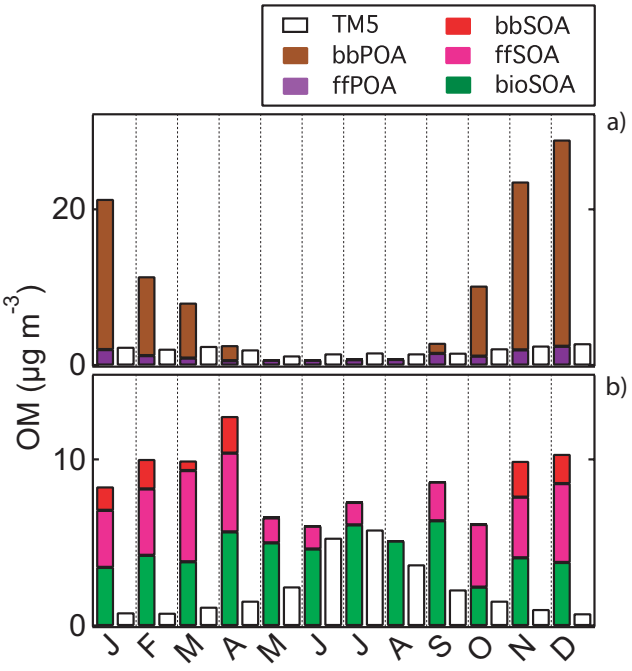

Fig. 4. Comparison of POA (panel **a**) and SOA (panel **b**) simulated by TM5 model (white boxes) and calculated based on ^{14}C and tracer concentrations.

$$SOA = 1.8 \cdot SOC_{bb} + 1.8 \cdot SOC_{bio} + 1.8 \cdot SOC_{ff} \quad (12)$$

AMS studies reported OM to OC ratios in the range 1.4–2.5, with higher values for oxidized organic aerosol and smaller values close to the emission sources (Aiken et al., 2008). In this study the ratio 1.4 was used for POA, and 1.8 for SOA.

The average OM, calculated as sum of SOA and POA, was 30.2 $\mu g\,m^{-3}$ and 10.6 $\mu g\,m^{-3}$, in winter and summer, respectively. These values are 10 to 17 % higher that the OM estimates presented in section 3.1, indicating that an accurate choice of the OM to OC ratio has to take into account the aerosol sources and their seasonality.

Figure 4 reports the comparison between POA and SOA simulated by TM5 model and estimated based on ^{14}C and tracer concentrations. The average POA derived from 2007 measurements was 19.0 and 1.8 $\mu g\,m^{-3}$ during winter and summer, respectively. The corresponding model calculated concentations were much lower (2.3 and 1.5 $\mu g\,m^{-3}$). The model simulated correctly POA concentration during the warmer months, while it underestimated during the rest of the year, likely due to the underestimation of biomass burning emission in the model; as highlighted in Fig. 4, the difference between source apportioned and model POA is roughly equivalent to biomass burning POA during the entire year.

SOA concentrations derived from source apportionment averaged 11.2 and 8.3 $\mu g\,m^{-3}$ in winter and summer, respectively. Although the model simulated correctly the biogenic SOA during June–August, it generally underestimated the

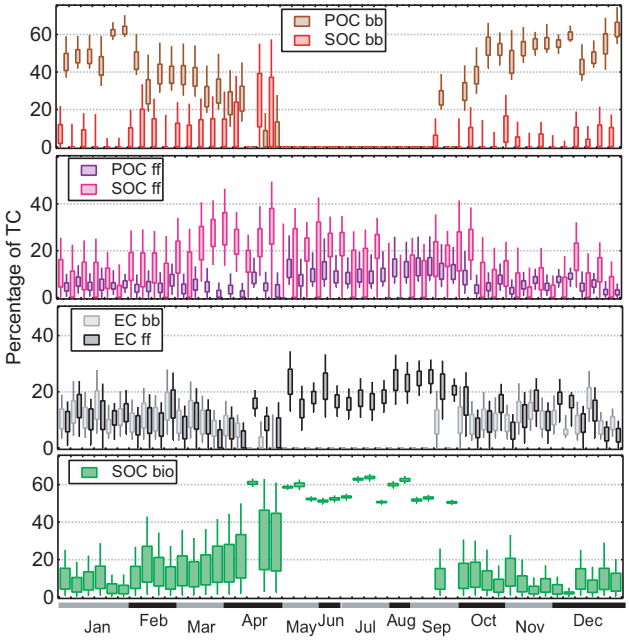

Fig. 5. Box-whisker plots of Quasi Monte Carlo simulation output for each day and each carbon source: POC_{bb} and SOC_{bb} (panel **a**), POC_{ff} and SOC_{ff} (panel **b**), EC_{bb} and EC_{ff} (panel **c**), and SOC_{bio} (panel **d**).

observations; the average model SOA was 0.8–1 µg m^{-3} and 3.2–3.4 µg m^{-3} in winter and summer, respectively. The difference between SOA observed and modeled was likely due to the underestimation of biomass burning and fossil source SOA from oxidation of IVOC, as well as underestimation of biogenic SOA during seasons other than summer.

3.4 Uncertainty analysis

The QMC calculations provide uncertainty estimates for each day and for each carbon source (Fig. 5). As a measure of the uncertainty we used the difference between the 95th and the 5th percentile of the solutions, corresponding roughly to $\pm 2\sigma$.

The uncertainty of POC_{bb} was usually comparable to that of SOC_{bb}; their average values were 15 % and 14 %, respectively. In a few cases (2 samples), SOC_{bb} uncertainty was higher than 25 %.

On the contrary, SOC_{ff} was characterized by a larger uncertainty compared to that of POC_{ff}, especially during winter. POC_{ff} uncertainty ranged between 6 and 20 % of TC, while SOC_{ff} uncertainty was often larger than 20 %. The highest uncertainties were associated with the lower concentrations during summer.

Both EC_{bb} and EC_{ff} were characterized by uncertainties smaller than 25 % during the entire year; their uncertainties averaged 10 % and 15 %, respectively.

The uncertainty of SOC_{bio} averaged 20 %; the highest uncertainties were observed during March and April. The lower SOC_{bio} uncertainties during summer were due to the negligible contributions of biomass burning aerosol. When biomass burning carbon was zero, EC to OC emission ratio of fossil fuel combustion was the only input parameters left to affect the output variability, together with the measurement uncertainties.

Neglecting the distinction between primary and secondary sources, the carbon emitted by biomass burning and fossil sources can be defined by the sum of the corresponding POC and SOC; this results in a reduction of uncertainty. On average, during winter OC_{bb} and OC_{ff} composed 50 % ± 7 % and 15 % ± 7 % of TC, respectively. During summer OC_{ff} represented 28 % ± 11 % of TC.

3.5 Seasonality of carbonaceous aerosol sources in comparison with other studies

We compared the seasonality of the source contribution to carbonaceous aerosols with apportionment data based on ^{14}C and tracer measurements performed at other European urban and rural locations (Table 5); data from remote sites are not used because these are dominated by biogenic emissions during the whole year (Gelencser et al., 2007).

OC_{bb}, OC_{ff}, and OC_{bio} in Table 5 are equal to the sum of primary and secondary OC. At Aveiro and K-puszta the reported OC_{bb} include only the primary contribution since no distinction was made between secondary biogenic and secondary wood burning OC. During summer the small contribution of OC and EC from biomass burning suggests that the secondary non-fossil OC was a good estimate of OC_{bio}. At Roveredo and Moleno OC_{bb} was assumed equal to non-fossil OC; in fact, aerosol mass spectra acquired during the same study compared very well with wood burning emission, pointing to an insignificant influence of biogenic OC (Szidat et al., 2007).

During winter OC and EC fractions emitted by biomass burning at the rural sites were, despite a large variability, consistently higher than the urban values. Conversely, the contribution of fossil carbonaceous aerosol did not show clear differences. The biomass burning carbon measured in Ispra compared well with the rural measurements and the fossil carbon fraction was consistently lower than that measured in urban sites.

A limited set of literature measurements were available during the summer season. The contribution of biomass burning was smaller than 11 % at all sites. The fossil carbon fraction at the urban sites was about two times larger than the rural fractions, while the biogenic carbon contribution was markedly more significant at the rural locations. The composition of carbonaceous aerosol in Ispra was comparable to that of urban sites (Zurich, Göteburg): Ispra aerosol had a larger fraction of fossil carbon aerosol relative to the rural locations (K-puszta and Aveiro).

Table 5. Percentage values of TC emitted by biomass burning (bb), fossil sources (ff) and biogenic sources (bio), together with average carbon concentration in $\mu g\,m^{-3}$ between brackets.

Site	Notes	OC_{bb}	EC_{bb}	OC_{ff}	EC_{ff}	OC_{bio}	Reference
Winter							
Aveiro	Rural	64[a](9.0)	11(1.5)	17(3.7)	2(0.3)		d
K-Puszta	Rural	40[a](4.3)	7(0.05)	21(2.2)	10(1.0)		d
Rao	Rural	31(0.6)	8(0.1)	28(0.5)	16(0.3)	17(0.3)	g
Roveredo	Rural	75[b] (12.6)	11(1.8)	4(0.5)	12(1.8)		f
Roveredo	Rural	62[b](6.9)	8(0.9)	21(1.6)	11(1.0)		f
Moleno	Rural	54[b](12.9)	4(1.0)	15(3.5)	30(6.7)		f
Zurich	Urban	29(6.9)	4(1.0)	25(5.4)	16(3.0)	46(4.5)	e
Göteborg	Urban	20(0.6)	3(0.09)	28(0.9)	26(0.8)	23(0.7)	g
Ispra	Rural	53(12.7)	11(2.5)	15(3.5)	12(2.6)	9(2.0)	This study
Summer							
Aveiro	Rural	7[a](0.3)	1(0.05)	7(0.3)	13(0.5)	65[c](2.6)	d
K-Puszta	Rural	6[a](0.3)	1(0.05)	9(0.3)	9(0.5)	69[c](3.7)	d
Zurich	Urban	8(0.3)	1(0.06)	24(1.1)	22(1.0)	46(2.1)	e
Göteborg	Urban	9(0.2)	2(0.04)	31(0.8)	15(0.4)	44(1.2)	g
Ispra	Rural	8(0.8)	1(0.2)	23(1.9)	18(1.2)	50(3.1)	This study

[a] Neglecting secondary OC, [b] Assuming non-fossil OC was OC_{bb} in winter, [c] Assuming secondary non-fossil OC was OC_{bio} in summer, [d] Gelencser et al. (2007), [e] Szidat et al. (2006), [f] Szidat et al. (2007), [g] Szidat et al. (2009).

The similarity of the source contribution in Ispra with rural sites in winter and with urban sites in summer was likely due to the influence of urban polluted air masses linked to lower atmospheric stability during summer. To verify this hypothesis, we further investigated the origin of polluted air masses with potential source contribution function (PSCF) for biomass burning and fossil carbonaceous aerosol.

3.6 Source regions

For the analysis of PSCF, the contribution of a specific carbon source was considered dominant when the percentage of TC was larger than the 75th percentile. We selected samples characterized by dominant contribution of POC_{ff} and POC_{bb}, limiting the investigation to primary carbon. This limitation was due to the smaller uncertainty of carbon from primary sources compared to secondary ones, and to the fact that the PSCF algorithm calculates the probability associated to primary pollutants transport excluding formation of secondary species.

The contribution of POC_{ff} to TC was more significant during summer, while the POC_{bb} fraction was higher during the colder months, especially November and December. As a consequence, the PSCF maps of POC_{ff} and POC_{bb} in Fig. 6 shows the influence regions typical of the winter and summer months, respectively. The smaller probability values of POC_{bb} are due to the lower mixing layer height during winter and the consequent lower influence of regional air masses.

The fossil carbon PSCF was higher in the grid cells close to Ispra and close to Milan, indicating a strong contribution from local sources and from regional sources mainly located in the urban areas of Milan and surroundings. The map shows also a likely contribution from the Po Valley region, to the south-east of Milan. This area is characterized by high density of population and industrial activities.

The highest PSCF values of POC_{bb} were observed in the surroundings close to Ispra. The remaining grid cells were characterized by probabilities smaller than 0.2, indicating that the biomass burning primary carbon observed in Ispra was mainly from local sources. The PSCF was larger than 0.1 in rural areas located to the south and south-east of Milan, while zero values were observed in the areas characterized by higher population density (Fig. 6c). This does not mean that the biomass burning emissions in urban areas were null, but that the influence of these emissions at the receptor site was negligible compared to the local emissions.

4 Conclusions

The sources of carbonaceous aerosols in Ispra, a European background site at the edge of the Po Valley, were investigated using macro-tracers (EC, OC, and levoglucosan), micro-tracers (arabitol and mannitol), and ^{14}C measurements. The concomitant use of tracers specific of a single source and measurements related to multiple sources constrained the source apportionment results. A Quasi-Monte

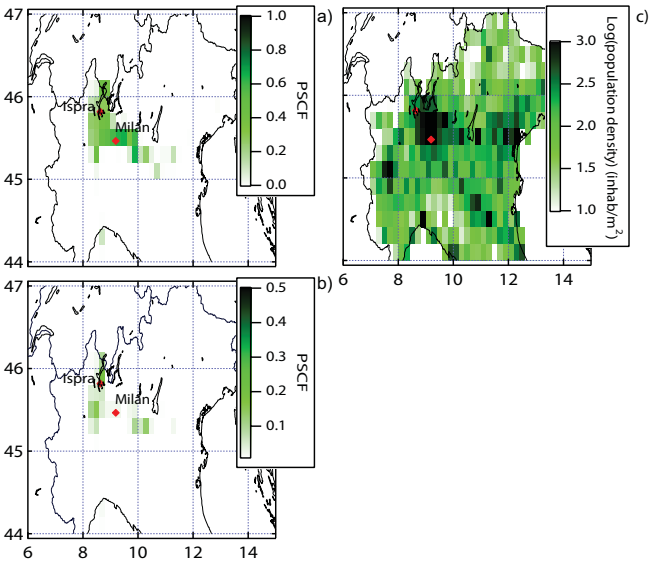

Fig. 6. PSCF maps of fossil fuel combustion (panel **a**) and biomass burning (panel **b**) aerosol; panel **(c)** shows northern Italy population density (ISTAT 2005).

Carlo approach was used to determine the most probable contributions of 8 source categories and the associated uncertainties. The resulting uncertainty of the emission factors, usually smaller than 20 % of TC, was much reduced compared to the range indicated a-priori assumptions derived from the literature.

Ispra is located to the north of the Po Valley and it is representative of rural/ near city areas. In Ispra anthropogenic activities, through fossil sources and biomass burning, contributed to 91 % and 50 % of TC during winter and summer, respectively. During the colder months, the largest fraction of the anthropogenic aerosol carbon was produced by biomass burning for residential heating (64 %). Environmental policies need to take into account the contribution of anthropogenic biomass burning to effectively reduce the concentration of fine particulate mass.

The comparison of source apportionment data with the global chemistry transport model TM5 showed the largest discrepancy in winter POA. The discrepancy was similar to the concentration of primary organic carbon emitted by biomass burning, whose contribution was not included in the model. Ispra, as other European rural areas, showed to be strongly affected by emissions from biomass fuel combustion, most likely wood burning; as a consequence, the availability of up-to-date wood burning emission inventories is a requirement to simulate correctly the OM distribution and eventually to evaluate the efficiency of aerosol reduction strategies. Moreover, TM5 model underestimated biogenic SOA and anthropogenic SOA from oxidation of intermediate volatile organic carbon components.

SOA from anthropogenic activities reported in this study represents a lower estimate of the actual SOA, due to the semi-volatile character of primary organic aerosol, which is currently not accurately described by the available emission factors. Still, the contribution of SOA from biomass burning and fossil sources burning was significant: SOA represented 30 % and 85 % of OM during winter and summer, respectively. These results agree with the high oxidized character of atmospheric organic aerosol reported by Aerodyne Aerosol Mass Spectrometer (AMS) measurements in anthropogenically influenced Northern Hemisphere areas (Zhang et al., 2007).

Biogenic SOA represented a significant percentage of OM both during winter (13 %) and summer (56 %).

In summer the site was affected by polluted air masses from the urban and industrialized areas located in the near Po Valley. The concentration of secondary biogenic aerosol during the same season was enhanced by anthropogenic primary aerosol, in agreement with earlier modeling studies (Tsigaridis and Kanakidou, 2007). The ultimate consequence of this would be that policies aiming to reduce aerosol species associated with positive warming (e.g. black carbon) would also reduce cooling secondary aerosol.

In closing, we showed that radiocarbon measurements, in combination with tracer analysis, provide unique constraints on the relative contributions of the major sources of carbonaceous aerosols, and that together with trajectory analysis, important information on the source regions can be determined. An expanding dataset is necessary to further understand the world wide contributions of sources to carbonaceous aerosol, improve emission inventories, and provide important information for emission reduction strategies.

Acknowledgements. This work was supported by the European Commission on the IP EUCAARI (036833-2) project. We gratefully acknowledge the EMEP team for their dedicated and reliable work during sample collection, and M. Duane for skillful assistance in the LC-MS analysis. The authors are very grateful to the referees for their extensive comments.

Edited by: A. Wiedensohler

References

Aiken, A. C., DeCarlo, P. F., Kroll, J. H., Worsnop, D. R., Huffman, J. A., Docherty, K. S., Ulbrich, I. M., Mohr, C., Kimmel, J. R., Sueper, D., Sun, Y., Zhang, Q., Trimborn, A., Northway, M., Ziemann, P. J., Canagaratna, M. R., Onasch, T. B., Alfarra, M. R., Prevot, A. S. H., Dommen, J., Duplissy, J., Metzger, A., Baltensperger, U., and Jimenez, J. L.: O/C and OM/OC Ratios of Primary, Secondary, and Ambient Organic Aerosols with High-Resolution Time-of-Flight Aerosol Mass Spectrometry, Environ. Sci. Technol, 42, 4478–4485, doi:10.1021/es703009q, 2008.

Antweiler, R. C. and Taylor, H. E.: Evaluation of Statistical Treatments of Left-Censored Environmental Data using Coincident

Uncensored Data Sets: I. Summary Statistics, Environ. Sci. Technol., 42, 3732–3738, 2008.

Bauer, H., Kasper-Giebl, A., Zibuschka, F., Hitzenberger, R., Kraus, G., and Puxbaum, H.: Determination of the carbon content of airborne fungal spores, Anal. Chem., 74, 91–95, 2002.

Bauer, H., Claeys, M., Vermeylen, R., Schueller, E., Weinke, G., Berger, A., and Puxbaum, H.: Arabitol and mannitol as tracers for the quantification of airborne fungal spores, Atmos. Environ., 42, 588–593, 2008a.

Bauer, H., Schueller, E., Weinke, G., Berger, A., Hitzenberger, R.and Marr, I., and Puxbaum, H.: Significant contributions of fungal spores to the organic carbon and to the aerosol mass balance of the urban atmospheric aerosol, Atmos. Environ., 42, 5542–5549, 2008b.

Birch, M. E. and Cary, R. A.: Elemental carbon-based method for monitoring occupational exposures to particulate diesel exhaust, Aerosol Sci. Technol., 25, 221–241, 1996.

Bowman, F. M. and Melton, J. A.: Effect of activity coefficient models on predictions of secondary organic aerosol partitioning, J. Aerosol Sci., 35, 1415–1438, 2004.

Boyle, P. P. and Tan, K. S.: Quasi-Monte Carlo methods, International AFIR Colloquium Proceedings, Australia, 1, 1–24, 1997.

Caflisch, R. E.: Monte Carlo and quasi Monte-Carlo methods, Acta Numerica, pp. 1–49, 1998.

Carlton, A. G., Pinder, R. W., Bhave, P. V., and Pouliot, G. A.: To what extent can biogenic SOA be controlled, Environ. Sci. Technol., 44, 3376–3380, 2010.

Cavalli, F., Viana, M., Yttri, K. E., Genberg, J., and Putaud, J.-P.: Toward a standardised thermal-optical protocol for measuring atmospheric organic and elemental carbon: the EUSAAR protocol, Atmos. Meas. Tech., 3, 79–89, doi:10.5194/amt-3-79-2010, 2010.

Colombi, C., Gianelle, V., Belis, C. A., and Larsen, B. R.: Determination of local source profile for soil dust, brake dust, and biomass burning sources, Chemical Engineering Transaction, 22, 233–238, doi:10.3303/CET1022,038, 2010.

Currie, L.: Contemporary particulate carbon, Proceedings of the international symposium on particulate carbon atmospheric life cycle, Warren, MI, USA, 13–14 Oct 1980, 1982.

Currie, L., Stafford, T., Sheffield, A., Klouda, G., Wise, S., Fletcher, R., Donahue, D., Jull, A., and T.W., L.: Microchemical and molecular dating, Radiocarbon, 31, 448–463, 1989.

Ding, X., Zheng, M., Edgerton, E. S., Jansen, J. J., and Wang, X.: Contemporary or Fossil Origin: Split of Estimated Secondary Organic Carbon in the Southeastern United States, Environ. Sci. Technol, 42, 9122–9128, 2008.

Dixon, R. W. and Baltzell, G.: Determination of levoglucosan in atmospheric aerosols using high performance liquid chromatography with aerosol charge detection, Journal of Chromatography, 1109, 214–221, 2006.

Docherty, K. S., Stone, E. A., Ulbrich, I. M., DeCarlo, P. F., Snyder, D. C., Schauer, J. J., Peltier, R. E., Weber, R. J., Murphy, S. M., Seinfeld, J. H., Grover, B. D., Eatough, D. J., and Jimenez, J. L.: Apportionment of Primary and Secondary Organic Aerosols in Southern California during the 2005 Study of Organic Aerosols in Riverside (SOAR-1), Environ. Sci. Technol, 42, 7655–7662, 2008.

Duane, M., Poma, B., Rembges, D., Astorga, C., and Larsen, B. R.: Isoprene and its degradation products as strong ozone precursors in Insubria, Northern Italy, Atmos. Environ., 36, 3867–3879, 2002.

El Haddad, I., Marchand, N., Wortham, H., Piot, C., Besombes, J.-L., Cozic, J., Chauvel, C., Armengaud, A., Robin, D., and Jaffrezo, J.-L.: Primary sources of $PM_{2.5}$ organic aerosol in an industrial Mediterranean city, Marseille, Atmos. Chem. Phys., 11, 2039–2058, doi:10.5194/acp-11-2039-2011, 2011.

Fabbri, D., Torri, C., Simoneit, B. R. T., Marynowski, L., Rushdi, A., and Fabiaska, M. J.: Levoglucosan and other cellulose and lignin markers in emissions from burning of Miocene lignites, Atmos. Environ., 43, 2286–2295, 2009.

Fine, P. M., Cass, G. R., and Simoneit, B. R. T.: Chemical Characterization of Fine Particle Emissions from the Fireplace Combustion of Woods Grown in the Northeastern United States, Environ. Sci. Technol, 35, 2665–2675, 2001.

Fine, P. M., Cass, G. R., and Simoneit, B. R. T.: Chemical Characterization of Fine Particle Emissions from the Fireplace Combustion of Woods Grown in the Southern United States, Environ. Sci. Technol., 36, 1442–1451, 2002.

Fine, P. M., Cass, G. R., and Simoneit, B. R. T.: Chemical Characterization of Fine Particle Emissions from the wood stove combustion of prevalent United States tree species, Environmental Engineer Science, 21, 705–721, 2004.

Fraser, M. P. and Lakshmanan, K.: Using levoglucosan as a molecular marker for the long-range transport of biomass combustion aerosols, Energy Environ Eng. S, 34, 4560–4564, 2000.

Gelencser, A., May, B., Simpson, D., Sanchez-Ochoa, A., Kasper-Giebl, A., Puxbaum, H., Caseiro, A., Pio, C., and Legrand, M.: Source apportionment of $PM_{2.5}$ organic aerosol over Europe: Primary/secondary, natural/anthropogenic, and fossil/biogenic origin, J. Geophys. Res., 112, D23S04, doi:10.1029/2006JD008, 2007.

Genberg, J., Stenström, K., Elfman, M., and Olsson, M.: Development of graphitization of µg-sized samples at Lund University., Radiocarbon, 52, 1270–1276, 2010.

Gery, M. W., Whitten, G. Z., and Killus, J. P.: Development and testing of the CBM-IV for urban and regional modelling, EPA-600/3-88-012, Tech. rep., US EPA, Research Triangle Park, 1989.

Gruening, C., Adam, M., Cavalli, F., Cavalli, P., Dell'Acqua, A., Martin Dos Santos, S., Pagliari, V., Roux, D., and Putaud, J. P.: JRC Ispra EMEP – GAW regional station for atmospheric research, 2008 report, Tech. rep., Joint Research Centre, Institute for Environment and Sustainability, 2009.

Hays, M. D., Geron, C. D., Linna, K. J., and Smith, N. D.: Speciation of gas–phase and particle emissions from burning of foliar fuels, Environ. Sci. Technol, 36, 2280–2295, 2002.

Henne, S., Brunner, D., Folini, D., Solberg, S., Klausen, J., and Buchmann, B.: Assessment of parameters describing representativeness of air quality in-situ measurement sites, Atmos. Chem. Phys., 10, 3561–3581, doi:10.5194/acp-10-3561-2010, 2010.

Hitzenberger, R., Petzold, A., Bauer, H., Ctyroky, P., Pouresmaeil, P., Laskus, L., and Puxbaum, H.: Intercomparison of thermal and optical measurement methods for elemental carbon and black carbon at an urban location., Environ. Sci. Technol, 40, 6377–6383, 2006.

Hodzic, A., Jimenez, J. L., Prévôt, A. S. H., Szidat, S., Fast, J. D., and Madronich, S.: Can 3-D models explain the observed fractions of fossil and non-fossil carbon in and near Mexico

City?, Atmos. Chem. Phys., 10, 10997–11016, doi:10.5194/acp-10-10997-2010, 2010.

IPCC: Fourth Assessment Record: Climate change 2007, Cambridge University Press, New York, 2007.

Jia, Y., Bhat, S., and Fraser, M. P.: Characterization of saccharides and other organic compounds in fine particles and the use of saccharides to track primary biologically derived carbon sources, Atmos. Environ., 44, 724–732, 2010.

Karl, M., Tsigaridis, K., Vignati, E., and Dentener, F.: Formation of secondary organic aerosol from isoprene oxidation over Europe, Atmos. Chem. Phys., 9, 7003–7030, doi:10.5194/acp-9-7003-2009, 2009.

Kourtchev, I., Copolovici, L., Claeys, M., and Maenhaut, W.: Characterization of atmospheric aerosols at a forestd site in central Europe, Environ. Sci. Technol, 43, 4665–4671, 2009.

Krol, M., Houweling, S., Bregman, B., van den Broek, M., Segers, A., van Velthoven, P., Peters, W., Dentener, F., and Bergamaschi, P.: The two-way nested global chemistry-transport zoom model TM5: algorithm and applications, Atmos. Chem. Phys., 5, 417–32, doi:10.5194/acp-5-417-2005, 2005.

Kuo, L. J., Herbert, B. E., and Louchouarn, P.: Can levoglucosan be used to characterize and quantify char/charcoal black carbon in environmental media?, Org. Geochem., 39, 1466–1478, 2008.

Kupiainen, K. and Klimont, Z.: Primary emissions of submicron and carbonaceous particles in Europe and the potential for their control, Tech. Rep. IR-04-079, International Institute for Applied System analysis IIASA, 2004.

Kupiainen, K. and Klimont, Z.: Primary emissions of fine carbonaceous particles in Europe, Atmos. Environ., 41, 2156–2170, 2007.

Lal, D. and Peters, B.: Cosmic ray produces radioactivity on the Earth, Handbuch der Physik, 46, 551–612, 1967.

Lanz, V. A., Prévôt, A. S. H., Alfarra, M. R., Weimer, S., Mohr, C., DeCarlo, P. F., Gianini, M. F. D., Hueglin, C., Schneider, J., Favez, O., D'Anna, B., George, C., and Baltensperger, U.: Characterization of aerosol chemical composition with aerosol mass spectrometry in Central Europe: an overview, Atmos. Chem. Phys., 10, 10453–10471, doi:10.5194/acp-10-10453-2010, 2010.

Lee, S., Wang, Y., and Russell, A. G.: Assessment of secondary organic carbon in the southestern United States: a review, Air Waste Manage., 60, 1282–1292, 2010.

Levin, I. and Kromer, B.: The tropospheric $^{14}CO_2$ level in midlatitudes of the northern hemisphere (1959–2003), Radiocarbon, 46, 1261–1272, 2004.

Levin, I. Hammer, S., Kromer, B., and Meinhardt, F.: Radiocarbon observations in atmopsheric CO_2: determining fossil fuel CO_2 over Europe using Jungfraujoch observations as background, Sci. Total Environ., 391, 211–216, 2008.

Lewis, C. W., Klouda, G. A., and Ellenson, W. D.: Radiocarbon measurenents of the biogenic contribution to summertime $PM_{2.5}$ ambient aerosol in Nashville, TN, Atmos. Environ., 38, 6053–6061, 2004.

Lonati, G., Giugliano, M., Butelli, P., Romele, L., and Tardivo, R.: Major chemical components of $PM_{2.5}$ in Milan (Italy), Atmos. Environ., 39, 1925–1934, 2005.

Ma, Y., Hays, M. D., Geron, C. D., Walker, J. T., and Gatari Gichuru, M. J.: Technical Note: Fast two-dimensional GC-MS with thermal extraction for anhydro-sugars in fine aerosols, Atmos. Chem. Phys., 10, 4331–4341, doi:10.5194/acp-10-4331-2010, 2010.

Matthias-Maser, S. and Jaenicke, R.: The size distribution of primary biological aerosol particles in the multiphase atmosphere, Aerobiologia, 16, 207–210, 2000.

Mohn, J., Szidat, S., Fellner, J., Rechberger, H., Quartier, R., Buchmann, B., and Emmenegger, L.: Determination of biogenic and fossil CO_2 emitted by waste incineration based on $^{14}CO_2$ and mass balances, Bioresource Technol., 99, 6471–6479, 2008.

Morgan, W. T., Allan, J. D., Bower, K. N., Highwood, E. J., Liu, D., McMeeking, G. R., Northway, M. J., Williams, P. I., Krejci, R., and Coe, H.: Airborne measurements of the spatial distribution of aerosol chemical composition across Europe and evolution of the organic fraction, Atmos. Chem. Phys., 10, 4065–4083, doi:10.5194/acp-10-4065-2010, 2010.

Nel, A.: Air pollution – related illness: Effects of particles, Science, 308, 5723, doi:10.1126/science.1108,752, 2005.

Nolte, C. G., Schauer, J. J., Cass, G. R., and Simoneit, B. R. T.: Highly polar organic compounds present in wood smoke and in the ambient atmosphere, Environ. Sci. Technol., 35, 1912–1919, 2001.

Pekney, N., Davidsonb, C. I., Zhouc, L., and Hopkec, P. K.: Application of PSCF and CPF to PMF-Modeled Sources of $PM_{2.5}$ in Pittsburgh, Aerosol Sci. Technol., 40, 952–961, 2004.

Pope, C. A. r. and Dockery, C. W.: Health effects of fine particulate air pollution: Lines that connect, J. Air Waste Manage., 56, 709–742, 2006.

Puxbaum, H., Caseiro, A., Sanchez-Ochoa, A., Kasper-Giebl, A., Claeys, M., Gelencser, A., Legrand, M., Preunkert, S., and Pio, C.: Levoglucosan levels at background sites in Europe for assessing the impact of biomass combustion on the European aerosol background, J. Geophys. Res, 112, D23S05, doi:10.1029/2006JD008,114, 2007.

Querol, X., Alastuey, A., Pey, J., Cusack, M., Pérez, N., Mihalopoulos, N., Theodosi, C., Gerasopoulos, E., Kubilay, N., and Koçak, M.: Variability in regional background aerosols within the Mediterranean, Atmos. Chem. Phys., 9, 4575–4591, doi:10.5194/acp-9-4575-2009, 2009.

Robinson, A., Donahue, N. M., Shrivastava, M. K., Weitkamp, E. A., Sage, A. M., Grieshop, A. P., Lane, T. E., Pierce, J. R., and Pandis, S.: Rethinking organic aerosols: semivolatile emissions and photochemical aging, Science, 315, 1259–1262, 2007.

Sanchez-Ochoa, A., Kasper-Giebl, A., Puxbaum, H., Gelencser, A., Legrand, M., and Casimiro, P.: Concentration of atmospheric cellulose: A proxy for plant debris across a west-east transect over Europe, J. Geophys. Res. Atmos., 112, D23S08, doi:10.1029/2006JD008180, 2007.

Schauer, J. J., Kleeman, M. J., Cass, G. R., and Simoneit, B. R. T.: Measurement of emissions from air pollution sources. 3 C1–C29 organic compounds from fireplace combstion of wood, Environ. Sci. Technol, 35, 1716–1728, 2001.

Schmidl, C., Bauer, H., Dattler, A., Hitzenberger, R., Weissenboeck, G., Marr, I. L., and Puxbaum, H.: Chemical characterization of particle emissions from burning leaves, Atmos. Environ., 42, 9070–9079, 2008a.

Schmidl, C., Marr, I. L., Caseiro, A., Kotianova, P., Berner, A., Bauer, H., Kasper-Giebl, A., and Puxbaum, H.: Chemical characterization of fine particle emissions from wood stove combustion of common woods growing in the mid-European Alpine regions, Atmos. Environ., 42, 126–141, 2008b.

Simoneit, B. R. T., Elias, V. O., Kobayashi, M., Kawamura, K., Rushdi, A., Medeiros, P. M., Rogge, W. F., and Didyk, B. M.: Sugars-Dominant Water-Soluble Organic Compounds in Soils and Characterization as Tracers in Atmospheric Particulate Matter, Environ. Sci. Technol, 38, 5939–5949, 2004.

Skog, G.: The single stage AMS machine at Lund University: Status Report, Nucl. Instrum. Methods, 259, 1–6, 2007.

Skog, G., Rundgren, M., and Sköld, P.: Status of the Single Stage AMS machine at Lund University after 4 years of operation, Nucl. Instrum. Methods, 268, 895–897, 2010.

Sobol, I. M.: The distribution of points in a cube and the approximate evaluation of integrals, USSR Computational mathematics and mathematical physics, 1967.

Stohl, A., Wotawa, G., Seibert, P., and Kromp-Kolb, H.: Interpolation Errors in Wind Fields as a Function of Spatial and Temporal Resolution and Their Impact on Different Types of Kinematic Trajectories, J. Appl. Meteorol., 34, 2149–2165, 1995.

Stohl, A., Forster, C., Frank, A., Seibert, P., and Wotawa, G.: Technical note: The Lagrangian particle dispersion model FLEXPART version 6.2, Atmos. Chem. Phys., 5, 2461–2474, doi:10.5194/acp-5-2461-2005, 2005.

Stone, E. A., Snyder, D. C., Sheesley, R. J., Sullivan, A. P., Weber, R. J., and Schauer, J. J.: Source apportionment of fine organic aerosol in Mexico City during the MILAGRO experiment 2006, Atmos. Chem. Phys., 8, 1249–1259, doi:10.5194/acp-8-1249-2008, 2008.

Szidat, S., Prévôt, A. S. H., Sandradewi, J., Alfarra, M. R., Synal, H.-A., Wacker, L., and Baltensperger, U.: Dominant impact of residential wood burning on particulate matter in Alpine valleys during winter, Geophys. Res. Lett., 34, L05820, doi:10.1029/2006GL028325, 2007.

Szidat, S., Ruff, M., Perron, N., Wacker, L., Synal, H.-A., Hallquist, M., Shannigrahi, A. S., Yttri, K. E., Dye, C., and Simpson, D.: Fossil and non-fossil sources of organic carbon (OC) and elemental carbon (EC) in Göteborg, Sweden, Atmos. Chem. Phys., 9, 1521–1535, doi:10.5194/acp-9-1521-2009, 2009.

Szidata, S., Jenka, T. M., Gaggelera, H. W., Synalc, H. A., Fissehab, R., Baltenspergerb, U., Kalbererd, M., Samburovad, V., Reimanne, S., Kasper-Gieblf, A., and Hajdas, I.: Radiocarbon (14C)-deduced biogenic and anthropogenic contributions to organic carbon (OC) of urban aerosols from Zurich, Switzerland, Atmos. Environ., 38, 4035–4044, 2004.

Tsigaridis, K. and Kanakidou, M.: Secondary organic aerosol importance in the future atmosphere, Atmos. Environ., 41, 4682–4692, cited By (since 1996) 37, 2007.

Tsigaridis, K., Krol, M., Dentener, F. J., Balkanski, Y., Lathiére, J., Metzger, S., Hauglustaine, D. A., and Kanakidou, M.: Change in global aerosol composition since preindustrial times, Atmos. Chem. Phys., 6, 5143–5162, doi:10.5194/acp-6-5143-2006, 2006.

Turpin, B. J. and Lim, H.-J.: Species contributions to $PM_{2.5}$ mass concentrations: revisiting common assumptions for estimating organic mass, Aerosol Sci. Technol., 35, 602–610, 2001.

Wan, E. C. and Yu, J. Z.: Determination of sugar compounds in atmospheric aerosols by liquid chromatography combined with positive electrospray ionization mass spectrometry, J. Chromatogr., 1107, 175–181, 2006.

Watson, J. G. and Chow, J. C.: Source characterization of major emission sources in the Imperial and Mexicali Valleys along the US/Mexico border, Sci. Total Environ., 276, 33–47, 2001.

Yttri, K. E., Aas, W., Torseth, K., Stebel, K., Tsyro, S., Simpson, D., Merckova, K., Wankmuller, R., Klimont, Z., Bergstrom, R. W., van der Gon, H. D., Holzer-Popp, T., and Schroedter-Homscheidt, M.: EMEP Status Report 4/2009 – Transboundary particulate matter in Europe, 2009.

Yu, X.-Y., Cary, R. A., and Laulainen, N. S.: Primary and secondary organic carbon downwind of Mexico City, Atmos. Chem. Phys., 9, 6793–6814, doi:10.5194/acp-9-6793-2009, 2009.

Zdráhal, Z., Oliveira, J., Vermeylen, R., Claeys, M., and Maenhaut, W.: Improved method for quantifying levoglucosan and related monosaccharide anhydrides in atmospherc aerosols and application to samples from urban and tropical locations, Environ. Sci. Technol., 36, 747–753, 2002.

Zeng, Y. and Hopke, P. K.: Study of the sources of acid precipitation in Ontario, Canada, Atmos. Environ., 23, 1499–1509, 1989.

Zhang, Q., Jimenez, J. L., Canagaratna, M. R., Allan, J. D., Coe, H., Ulbrich, I., Alfarra, M. R., Takami, A., Middlebrook, A. M., Sun, Y. L., Dzepina, K., Dunlea, E., Docherty, K., DeCarlo, P. F., Salcedo, D., Onasch, T., Jayne, J. T., Miyoshi, T., Shimono, A., Hatakeyama, S., Takegawa, N., Kondo, Y., Schneider, J., Drewnick, F., Borrmann, S., Weimer, S., Demerjian, K., Williams, P., Bower, K., Bahreini, R., Cottrell, L., Griffin, R. J., Rautiainen, J., Sun, J. Y., Zhang, Y. M., and Worsnop, D. R.: Ubiquity and dominance of oxygenated species in organic aerosols in anthropogenically-influenced Northern Hemisphere midlatitudes, Geophys. Res. Lett., 34, L13801, doi:10.1029/2007GL029979, 2007.